analytical chemistry

Article

pubs.acs.org/ac

Multicolor Fluorescent Biosensor for Multiplexed Detection of DNA

Rong Hu,[†,‡,§] Tao Liu,[†,§] Xiao-Bing Zhang,*[,†] Shuang-Yan Huan,[†] Cuichen Wu,[‡] Ting Fu,[†] and Weihong Tan*[,†,‡]

[†]Molecular Science and Biomedicine Laboratory, State Key Laboratory of Chemo/Biosensing and Chemometrics, College of Chemistry and Chemical Engineering, College of Biology, Collaborative Innovation Center of Molecular Engineering for Theranostics, Hunan University, Changsha 410082, P.R. China

[‡]Center for Research at the Bio/Nano Interface, Department of Chemistry and Department of Physiology and Functional Genomics, Shands Cancer Center, UF Genetics Institute, and McKnight Brain Institute, University of Florida, Gainesville, Florida 32611-7200, United States

Supporting Information

ABSTRACT: Development of efficient methods for highly sensitive and rapid screening of specific oligonucleotide sequences is essential to the early diagnosis of serious diseases. In this work, an aggregated cationic perylene diimide (PDI) derivative was found to efficiently quench the fluorescence emission of a variety of anionic oligonucleotide-labeled fluorophores that emit at wavelengths from the visible to NIR region. This broad-spectrum quencher was then adopted to develop a multicolor biosensor via a label-free approach for multiplexed fluorescent detection of DNA. The aggregated perylene derivative exhibits a very high quenching efficiency on all ssDNA-labeled dyes associated with biosensor detection, having efficiency values of 98.3 ± 0.9%, 97 ± 1.1%, and 98.2 ± 0.6% for FAM, TAMRA, and Cy5, respectively. An exonuclease-assisted autocatalytic target recycling amplification was also integrated into the sensing system. High quenching efficiency combined with autocatalytic target recycling amplification afforded the biosensor with high sensitivity toward target DNA, resulting in a detection limit of 20 pM, which is about 50-fold lower than that of traditional unamplified homogeneous fluorescent assay methods. The quencher did not interfere with the catalytic activity of nuclease, and the biosensor could be manipulated in either preaddition or postaddition manner with similar sensitivity. Moreover, the proposed sensing system allows for simultaneous and multicolor analysis of several oligonucleotides in homogeneous solution, demonstrating its potential application in the rapid screening of multiple biotargets.

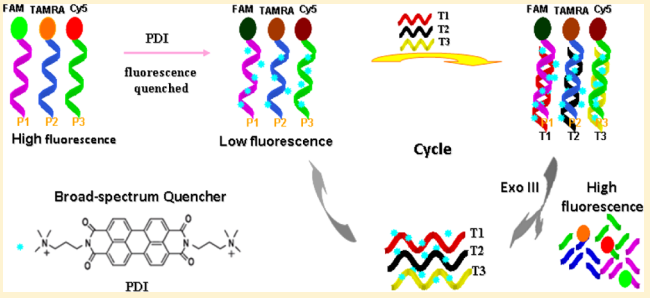

The development of efficient methods for highly sensitive and rapid detection of sequence-specific oligonucleotides is essential for the early diagnosis of serious diseases. In particular, insertion/deletion variations in oligonucleotides can lead to the onset of certain cancers and some genetic diseases[1−3] as well as individual differences in drug metabolism.[4,5] On the basis of their simplicity, low-cost, high sensitivity, rapid analysis, and little proclivity to sample or cell damage, fluorescent methods have attracted much attention and have been widely applied for the detection of various biomolecules.[6−9] In the past decade, the design of fluorescent biosensors for oligonucleotides has also attracted considerable attention.[10−12] Note that, although polymerase chain reaction (PCR) is the gold standard for DNA detection (for example, Banada et al. reported an assay based on PCR for highly sensitive detection of *Staphylococcus aureus* directly from patient blood[13]), specific and expensive equipment is required. Most fluorescent biosensors are based on the use of a nonfluorescent quencher, which endows the sensing system with high sensitivity. To date, the most frequently used commercial quenchers are small organic molecules. However, they usually require conjugation on the probe through tedious modifying steps, and they suffer from low, or variant, quenching efficiency for fluorophores that emit at different wavelengths.[14,15]

A variety of nanomaterial-based quenchers, including carbon nanomaterials and gold nanoparticles (AuNPs), have been developed with high quenching efficiency.[16−19] For example, AuNPs are able to quench FAM with a quenching efficiency 100-fold higher than that of organic quenchers.[20] Nevertheless, these AuNP-based methods generally exhibit poor salt and thermal stability, thus limiting their practical applications.[20,21] It has also been proven that the fluorescence of different kinds of dyes can be efficiently quenched by carbon nanotubes (CNTs) or graphene. However, proteins and other biomolecules are prone to nonspecific adsorption on CNTs or graphene, which may inhibit the activity of these biomolecules to some extent.[22−24] Chen et al. reported a broad-spectrum nanoquencher by incorporating a series of dark quenchers into mesoporous silica nanoparticles (MSNs),[25] which could

Received: February 13, 2014
Accepted: April 14, 2014
Published: April 14, 2014

   dx.doi.org/10.1021/ac500618v | Anal. Chem. 2014, 86, 5009−5016

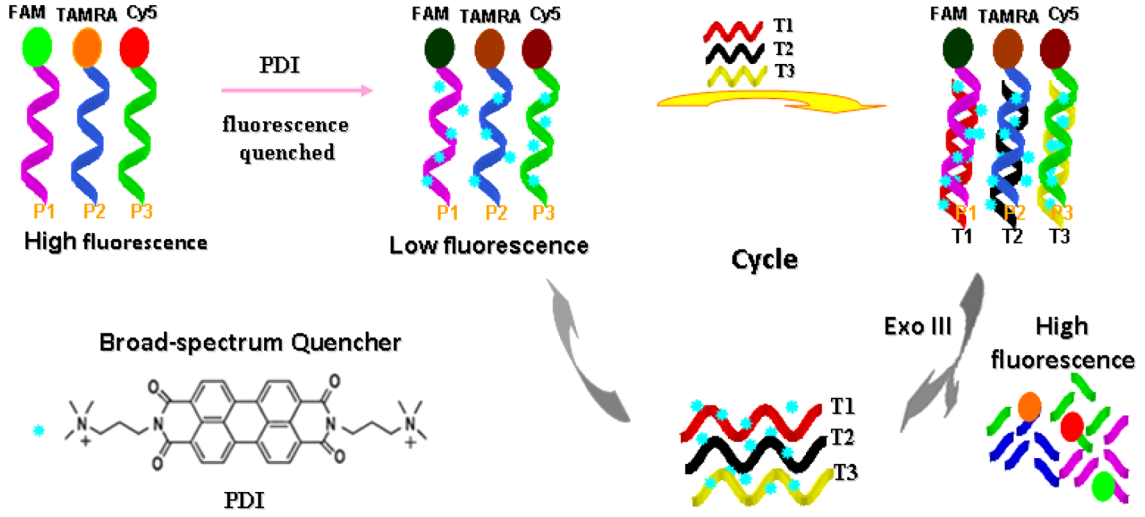

Figure 1. Schematic illustration of the aggregated perylene-based broad-spectrum quencher with the Exo III-assisted enzymatic recycling amplification strategy for amplified multiplexed analysis of DNA.

efficiently quench a broad range of visible and near-infrared (NIR) fluorophores. However, tedious steps were required to prepare the reported nanoquencher. The development of an easily synthesized, broad-spectrum fluorescent quencher with high quenching efficiency, as well as high biocompatibility and stability, is therefore highly desirable.

Perylene diimide (PDI) derivatives have been reported as excellent fluorophores because of their high fluorescence quantum yield and photostability, high thermal stability, and excellent chemical inertness.[26] A cationic perylene diimide derivative (PDI, Figure 1) was reported to associate with single-stranded DNA (ssDNA) with efficient fluorescence quenching.[27] In this work, we first report that cationic aggregated and quenched perylene can act as a broad-spectrum and label-free quencher via strong electrostatic interactions. When aggregated on oligonucleotides, PDI is able to efficiently quench a variety of adjacent conjugated anionic fluorophores that emit over a wide wavelength range from the visible to NIR region. This broad-spectrum quencher was then employed to develop a multicolor biosensor for multiplexed fluorescent detection of DNA via a label-free approach. Aggregated PDI exhibits a very high quenching efficiency on all ssDNA-labeled fluorophores of the sensing system, allowing low background fluorescence and therefore low detection limits.

Exonuclease III (Exo III) is a sequence-independent enzyme that does not require a specific recognition site and can catalyze the stepwise removal of mononucleotides from 3′-hydroxyl termini of double-stranded DNA (dsDNA).[28−31] Therefore, an Exo III-assisted autocatalytic target recycling amplification was also integrated into the sensing system. Formation of dsDNA through the hybridization of the target with the linear probe leads to the digestion of dsDNA by Exo III and subsequent release of the target, which can repeatedly hybridize with new linear probes, leading to the digestion of abundant dsDNAs by Exo III.[31] High quenching efficiency combined with autocatalytic target recycling amplification afforded the biosensor high sensitivity toward target DNA, resulting in a detection limit of 20 pM, which is about 50-fold lower than that of traditional unamplified homogeneous fluorescent assay methods. Moreover, the biosensor could discriminate perfectly matched target DNA from mismatched DNA. Simultaneous and multicolor analysis of several oligonucleotides in homogeneous solution was also achieved by the proposed sensing system, thus demonstrating its potential application in the rapid screening of multiple biotargets. Finally, our designed strategy is universal and may be useful in the detection of other target DNA analytes.

EXPERIMENTAL SECTION

Reagents and Apparatus. DNA oligonucleotides used in this work were synthesized and purified by SangonBiotechnology Co., Ltd. (Shanghai, China), and their sequences are shown in Table S1 in the Supporting Information. Perylenetetracarboxylicdianhydride and *N*,*N*-dimethyl-1,3-propanediamine were purchased from Alfa Aesar. Methyl iodide and other compounds were obtained from Shanghai Chemical Reagent Co. (Shanghai, China). All chemicals were of analytical grade and used without further purification. The nuclease exonuclease III was purchased from New England Biolabs. All solutions were prepared in Milli-Q water (resistance >18 MΩ cm) from a Millipore system. All fluorescence measurements were carried out on a Fluoromax-4 spectrofluorometer (HORIBA JobinYvon, Edison, NJ). All measurements were carried out at room temperature unless stated otherwise.

Quenching Efficiency Investigation. Different concentrations of PDI were added to solutions containing 10 μL of 1 μM various fluorophore-labeled DNA (FAM-P1, TAMRA-P2, Cy5-P3). In all cases, the total volume of the reaction solution was 100 μL. After incubation for 10 min, the fluorescence was measured by FluoroMax-4 spectrofluorometer (HORIBA JobinYvon, Edison, NJ).

Procedures for DNA Detection. For DNA detection, 100 nM of TAMRA DNA probe was first incubated with 14 μL of 10 μM PDI at room temperature in a buffer solution (10 mM 1, 3-bis (tris (hydroxymethyl)methylamino)propane-HCl, 10 mM $MgCl_2$, 1 mM dithiothreitol (DTT), pH 7.0). After 10 min, different concentrations of target DNA and 4 U of endonuclease Exo III were added to the sample solution. Then the mixture was incubated at 37 °C for 0.5 h, and the FluoroMax-4 spectrofluorometer was used to record the fluorescence intensity change at 583 nm (λ_{exc} = 559 nm).

Multiplex DNA Simultaneous Detection. FAM DNA probe (P1), TAMRA DNA probe (P2), and Cy5 DNA probe (P3) were first incubated with 20 μL of 10 μM PDI at room

dx.doi.org/10.1021/ac500618v | *Anal. Chem.* 2014, 86, 5009−5016

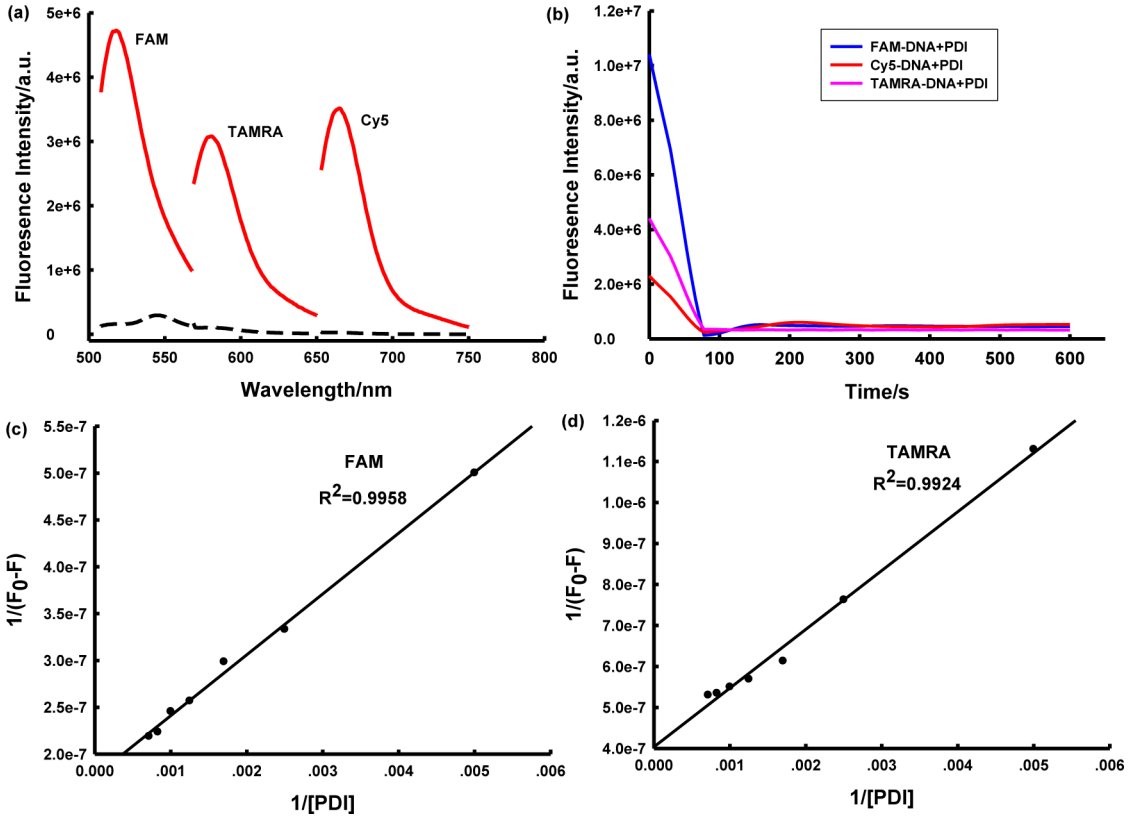

Figure 2. (a) Fluorescence spectra of 100 nM P1 (left), P2 (middle), and P3 (right) in the absence (red) and presence (black) of PDI. (b) Fluorescence kinetics curves of 100 nM P1, P2, and P3 upon addition of 1 μM of PDI. Lineweaver–Burk plots for 100 nM (c) P1 and (d) P2. F_0 and F are the fluorescence intensity of the fluorophore in the absence and presence of PDI, respectively. The data for P1 are recoded with the excitation and emission wavelength of 494 and 520 nm, respectively. The data for P2 are recoded with the excitation and emission wavelength of 559 and 583 nm, respectively.

temperature. After 10 min, DNA samples and 4 U of endonuclease Exo III were added to the sample solution. Then, the mixtures were incubated at 37 °C for 0.5 h. The FluoroMax-4 spectrofluorometer was used to record the fluorescence intensity change.

RESULTS AND DISCUSSION

Design Strategy. A multiplexed bioassay platform was constructed for simple, sensitive, and multiplex analysis of target DNA sequences. The design scheme is shown in Figure 1. The 5′-end of the probe DNA (P1, P2, and P3, complementary to target DNA T1, T2, and T3, respectively) is labeled with fluorophores FAM, TAMRA, or Cy5. The perylene derivative (PDI) aggregates on the probe and quenches the fluorescence of the fluorophores. Thus, the fluorophore-labeled ssDNAs exhibit low fluorescence emission as a result of their efficient quenching. Upon addition of the target ssDNA, the fluorophore-labeled ssDNA probes hybridize to target DNA to form duplex DNA structures with blunt-ended 3′-hydroxyl termini, so that the duplex DNA structure will become the substrate for Exo III cleavage. Then, Exo III catalyzes the stepwise removal of mononucleotides from the blunt 3′ termini, resulting in the release of the target and fluorophore. The released fluorophores are no longer quenched by the aggregated perylene derivative, thus increasing the fluorescence intensity. Because the duplex DNA probe can be stepwise removed by Exo III, the target DNA is released and hybridizes with another fluorescently labeled DNA, initiating the next round of cleavage. One target DNA sequence can initiate numerous probe digestions, leading to a highly sensitive DNA detection method. By monitoring the increase in fluorescence intensity, the target can be detected with very high sensitivity. Therefore, a multicolor sensor for analysis of multiple DNAs in homogeneous solution can be developed when different probes with corresponding fluorophores are used.

The fluorescence quenching ability of aggregated PDI was first investigated with the fluorophore-labeled ssDNA. As shown in Figure 2a, upon addition of PDI to the solution of fluorescein FAM-, TAMRA-, or Cy5-labeled ssDNA (P1, P2, or P3), the fluorescence intensity greatly decreased. More than 98% of FAM's fluorescence was quenched with 1.2 μM of PDI in the solution. The quenching efficiencies on the fluorescence of FAM, TAMRA, and Cy5 could reach to 98.3% ± 0.9%, 97 ± 1.1%, and 98.2% ± 0.6%, respectively. This result reveals that aggregated PDI can efficiently quench the fluorescence of fluorophores labeled on ssDNA. Moreover, the fluorescence intensity reaches a steady value within only 2 min (Figure 2b), indicating the rapid aggregation and quenching of PDI on ssDNA.

Fluorescence quenching usually consists of static quenching and dynamic quenching. Dynamic quenching can be described by Stern–Volmer's equation (eq 1), while static quenching can be described by the Lineweaver–Burk equation (eq 2)

$$F_0/F = 1 + K_{SV}c_q \quad (1)$$

$$1/(F_0 - F) = 1/F_0 + K_{LB}/(F_0c_q) \quad (2)$$

dx.doi.org/10.1021/ac500618v | Anal. Chem. 2014, 86, 5009–5016

where F_0 and F are the fluorescence intensities of the fluorophores in the absence and in the presence of a quencher (aggregated PDI), respectively, c_q is the concentration of the quencher, K_{SV} is the dynamic quenching constant, and K_{LB} is the static quenching constant.[32−37] By increasing the concentration of aggregated PDI, the change of fluorescence intensity for fluorophore-labeled ssDNA demonstrated a linear Lineweaver−Burk plot (Figure 2c,d and Figure S1 in the Supporting Information). Thus, the fluorescence quenching followed a static quenching mechanism. Moreover, the Stern−Volmer plot also showed good correlation, indicating a dynamic quenching mechanism (Figure S2 in the Supporting Information). Therefore, the fluorescence quenching mechanism of PDI followed both static and dynamic processes.[37,38] Since ssDNA is a polyanion, it can induce aggregation of the positively charged aggregated PDI via electrostatic interactions. Therefore, the quenching mechanism appears to be a function of the strong interaction between aggregated PDI and DNA sequences, and under these conditions, the fluorescence quenching of fluorophore-labeled DNA can be said to occur by strong intermolecular hydrophobic and $\pi-\pi$ stacking interactions (Figure S3 in the Supporting Information).

We further studied the behaviors of the TAMRA DNA probe P2−PDI complex in the absence and presence of target T2 by collecting the fluorescence emission spectra. A 4.5-fold fluorescence increase was detected upon addition of 100 nM target T2 (Figure S4 in the Supporting Information). The pH effect of buffer solution (50 mM Tris-HCl, 100 mM NaCl) on the affinities of aggregated PDI toward ssDNA and dsDNA was also investigated. As shown in Figure S5 in the Supporting Information, as pH changed, the change of PDI affinity between ssDNA and dsDNA was negligible. The different affinities of aggregated PDI toward ssDNA and dsDNA broadened the opportunities for the application of aggregated PDI in homogeneous fluorescence sensing of analytes.

In order to achieve the best sensing performance, the concentrations of perylene derivative and Exo III were optimized. Experimental results showed that a concentration of 1.4 μM perylene derivative and 4 U of Exo III could provide maximum signal-to-noise ratio (S/N) for the sensing system (Figures S6 and S7 in the Supporting Information), and these values were chosen as optimized conditions for further investigation.

To assess the amplification function of endonuclease, the target-induced fluorescence enhancements in the presence and absence of exonuclease III were then studied. The amplification assay was prepared by mixing TAMRA DNA probe P2 with perylene derivative. Then target T2 (50 nM) and Exo III (4 U) were added, and the mixture was incubated at 37 °C for 30 min. The exonuclease-assisted autocatalytic target recycling amplification led to a dramatic increase in the final fluorescence intensity upon the addition of the target T2. As shown in Figure 3A, in the absence of endonuclease, only a (210 ± 12)% signal increase was observed upon the addition of 50 nM target T2. In contrast, under the same conditions, the introduction of exonuclease III for signal amplification provided a (1446 ± 21)% fluorescence enhancement. These results confirm that this assay can provide significant signal amplification for DNA detection.

We next determined whether two approaches (preaddition and postaddition) would influence the accurate quantification of target DNA. An aliquot of PDI suspension was first added to the solution containing the TAMRA DNA probe P2, followed

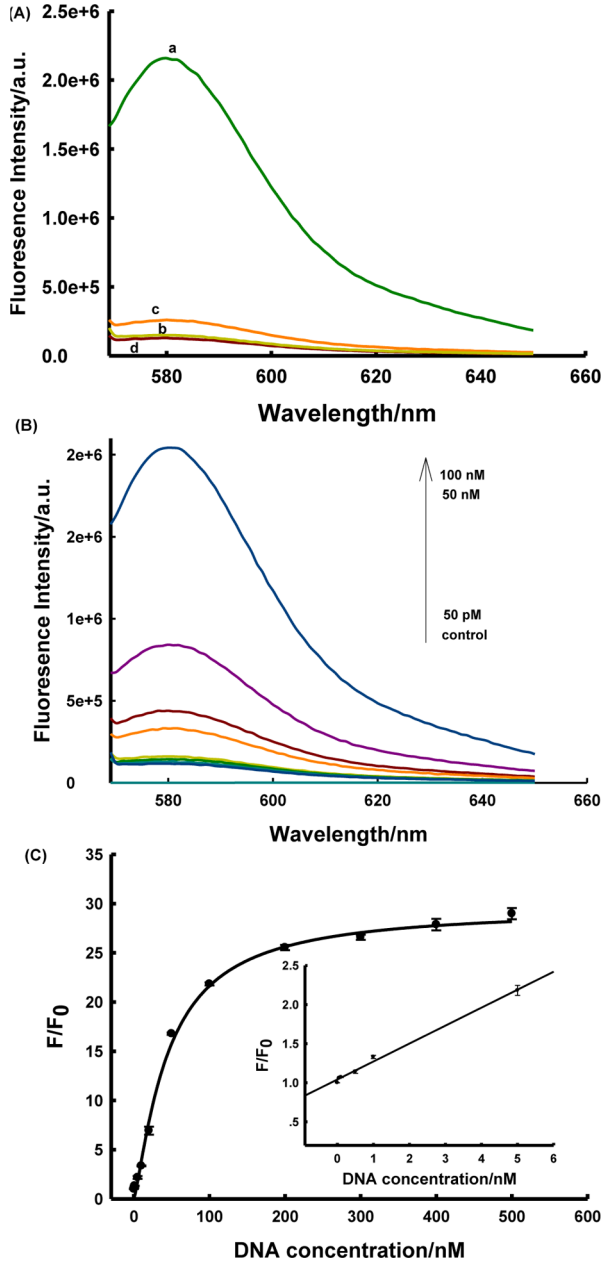

Figure 3. (A) Fluorescence spectra correspond to sensing systems (d) in the absence of target T2 or (c) in the presence of target T2 and the biosensor after Exo III amplification (b) in the absence of target T2 or (a) in the presence of target T2. The addition of Exo III led to a large increase of the fluorescence signal with target T2 concentration of 50 nM. (B) Fluorescence spectra of assay systems with "postaddition" strategy at various concentrations of DNA corresponding to data in the graph. (C) The relationship between fluorescence enhancement and target concentration. Inset shows the responses of sensing system to DNA at low concentration. F_0 and F are the fluorescence intensity of the sensor in the absence and presence of target, respectively. The data were recorded with excitation and emission wavelengths of 559 and 583 nm, respectively, and from at least three independent experiments.

by adding target T2 and appropriate concentrations of Exo III and incubating at 37 °C for 0.5 h. The above-mentioned method is the postaddition approach. In contrast, a "preaddition" approach was also performed by first mixing P2 probe and target T2 (or control) with Exo III and then PDI was

dx.doi.org/10.1021/ac500618v | Anal. Chem. 2014, 86, 5009−5016

added after the completion of the digestion reaction (Figure S8 in the Supporting Information). Compared with the preaddition approach, the postaddition approach is simple and easy to accomplish and could provide *in situ* and real-time information for targets. One can observe that the fluorescence intensity increased gradually with the increasing DNA concentration, irrespective of whether the postaddition (Figure 3B) or preaddition approach (Figure 4) were used. Figure 3C

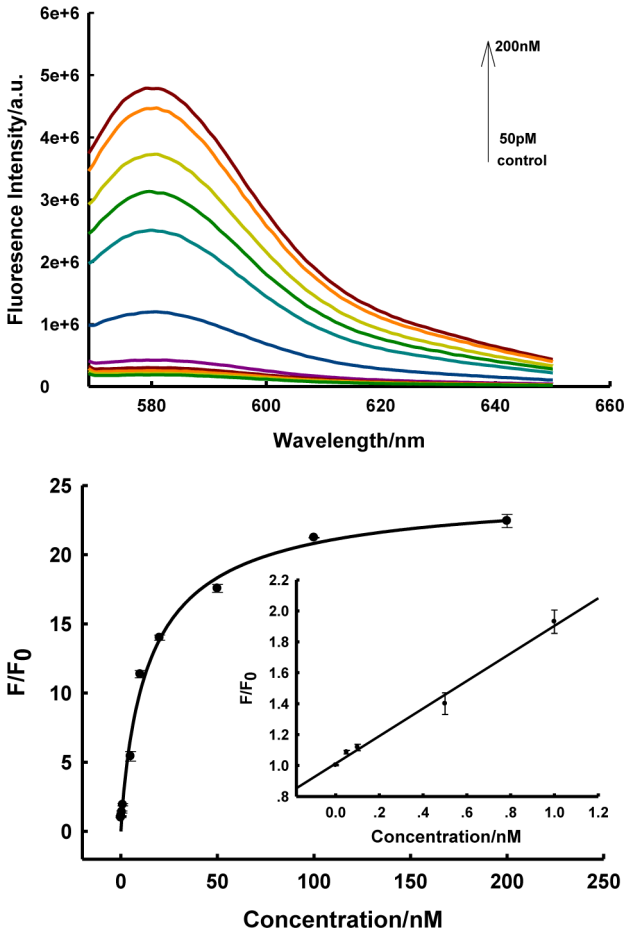

Figure 4. (a) Fluorescence spectra of assay systems with "preaddition" strategy at various concentrations of DNA corresponding to data in the graph. (b) The relationship between fluorescence enhancement and the target concentration. Inset shows the responses of the sensing system to DNA at low concentration. F_0 and F are the fluorescence intensity of the sensor in the absence and presence of target, respectively. The data were recorded with excitation and emission wavelengths of 559 and 583 nm, respectively, and from at least three independent experiments.

shows that the dynamic range of the amplified sensing system was from 50 pM to 5 nM and that the detection limit was 20 pM (S/N = 3). Almost the same detection limit for DNA detection was obtained from either of these approaches, suggesting that the aggregated perylene derivative did not affect the activity of the nucleases. Thus, we performed the postaddition strategy in the experiments. A Pd nanowire with Exo III-assisted target recycling, also using the postaddition approach for highly sensitive nucleic acid detection, has been reported for DNA detection. However, sensitivity is poor with a detection limit of only 0.3 nM. Compared with other strategies used for homogeneous fluorescence multiplexed detection of DNA, the perylene derivative-based assay shows shorter assay time and a comparable, or even lower, detection limit (Table S2, Supporting Information).

In contrast, control experiments for the biosensor with DNA at various concentrations in the absence of endonuclease were also carried out, with a detection limit of only 2 nM observed (Figure 5) and sensitivity almost 2 orders of magnitude poorer

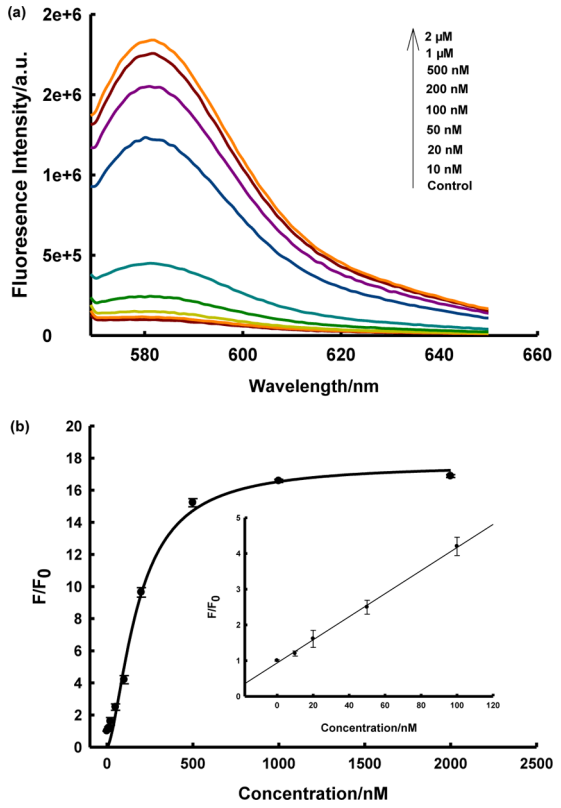

Figure 5. (a) Fluorescence spectra of assay systems without Exo III amplification at various concentrations of DNA corresponding to data in the graph. (b) The relationship between fluorescence enhancement and the target concentration. Inset shows the responses of sensing system to DNA at low concentration. F_0 and F are the fluorescence intensity of the sensor in the absence and presence of target, respectively. The data were recorded with excitation and emission wavelengths of 559 and 583 nm, respectively, and from at least three independent experiments.

than that of the Exo III-catalyzed amplified method. These results indicate that the introduction of nuclease remarkably improved the sensitivity of the biosensor.

To demonstrate that broad-spectrum quenching capability, as herein proposed, could be used for amplified multiplexed target detection in a homogeneous solution, the multiplexed detection ability was further investigated. Three probes, P1, P2, and P3, were labeled with FAM, TAMRA, or Cy5, respectively. Significant dye-to-dye energy transfer was avoided by choice of these three fluorophores, which were individually excited at 494, 559, and 643 nm, emitting blue (520 nm), orange (583 nm), and red (670 nm) colors, respectively. Using PDI for multiple fluorophores and Exo-III-assisted amplification, we could distinguish highly similar DNA sequences and detect them simultaneously. It is expected that fluorophore-labeled ssDNA probes hybridize to corresponding target DNA to form a duplex DNA structure in the presence of the corresponding target DNA. The addition of exonuclease induces the cleavage

dx.doi.org/10.1021/ac500618v | *Anal. Chem.* 2014, 86, 5009−5016

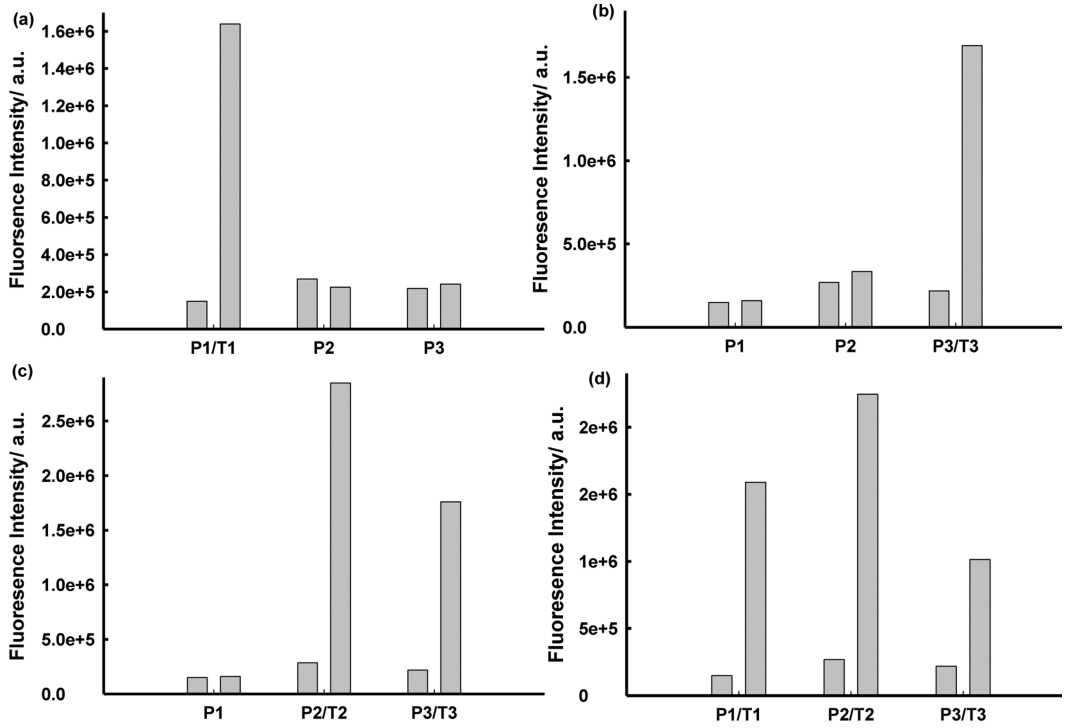

Figure 6. Multiplex and sequence-selective analysis of DNA. The measurement conditions of FAM were excitation at 494 nm and emission at 520 nm. The measurement conditions of TAMRA were excitation at 559 nm and emission at 583 nm. The measurement conditions of Cy5 were excitation at 645 nm and emission at 670 nm.

of the corresponding fluorophore-labeled DNA probe, resulting in significant fluorescence enhancement of the corresponding fluorophore (FAM, TAMRA, or Cy5). As shown in Figure 6a, upon the addition of target T1, signal increase was observed only in the FAM channels, while a weak signal change was observed in the TAMRA and Cy5 channels. The method could also be used for the specific detection of target T2 or target T3 (Figure 6b). The simultaneous detection of the two DNAs was also carried out. When target T2 and target T3 were added to the mixed solution, the fluorescence enhancements for both TAMRA and Cy5 channels were observed (Figure 6c). At the same time, the fluorescence intensity of FAM did not change greatly. Therefore, our method can be used for simultaneous detection of target T1 and target T2, target T1 and target T3, target T2 and target T3 pairs, respectively. Moreover, when all targets were present, fluorescence was observed in all three detection channels (Figure 6d). The sensitivity and dynamic range of the multiplexed sensing platform was also evaluated. Figure 7 represents the fluorescence intensity of the multiplexed sensing platform toward target T1 and target T2 with different concentrations. One can observe that the fluorescence intensity increased gradually with the increase of target T1 and target T2 concentrations. Figure 7b shows that the dynamic range of the amplified multiplexed sensing system for target T1 was from 50 pM to 10 nM and that the detection limit was 20 pM (S/N = 3). Figure 7d shows that the dynamic range of the amplified multiplexed sensing system for target T2 was from 50 pM to 5 nM and that the detection limit was 20 pM (S/N = 3). These results clearly demonstrate the feasibility of our strategy for multiplexed detection of DNA.

To investigate the specificity of the sensing system, we compared the fluorescence response induced by DNA strands containing single-base- and two-base-mismatched oligonucleotides with that of target T2. All results are displayed in Figure S9 in the Supporting Information. It was found that the target DNA T2 with the perfectly matched sequence induced 13-fold fluorescence enhancement. However, 4.6-fold and 2-fold fluorescence increase was observed when the DNA targets contained single-base-mismatched and two-base-mismatched oligonucleotides, respectively. These results demonstrated that this DNA sensing system can be used to discriminate perfectly matched from mismatched DNA targets.

In conclusion, it has been demonstrated that cationic aggregated and quenched perylene (PDI) can act as a broad-spectrum and label-free quencher via strong electrostatic interactions. It efficiently quenches a variety of adjacent anionic oligonucleotide-labeled fluorophores that emit over a wide wavelength range from the visible to NIR region. By combining aggregated perylene derivative broad-spectrum quenching with the Exo III-assisted autocatalytic target recycling amplification strategy, we proposed a sensitive and multiplexed analytical platform with postaddition approach for target DNA detection. The quencher did not interfere with the catalytic activity of the nuclease, and the biosensor could be manipulated in either preaddition or postaddition manner with similar sensitivity. High quenching efficiency combined with autocatalytic target recycling amplification afforded the biosensor high sensitivity toward target DNA. The present amplification sensing system for the DNA detection has a dynamic range from 50 pM to 2.0 μM with a detection limit of 20 pM (S/N = 3), which is about 50-fold lower than that of traditional unamplified homogeneous assays. Moreover, the biosensor could discriminate perfectly matched target DNA from mismatched DNA. Simultaneous and multicolor analysis of several oligonucleotides in homogeneous solution was also achieved by the proposed sensing system, thus demonstrating its potential application in the rapid screening of multiple biotargets.

dx.doi.org/10.1021/ac500618v | *Anal. Chem.* 2014, 86, 5009−5016

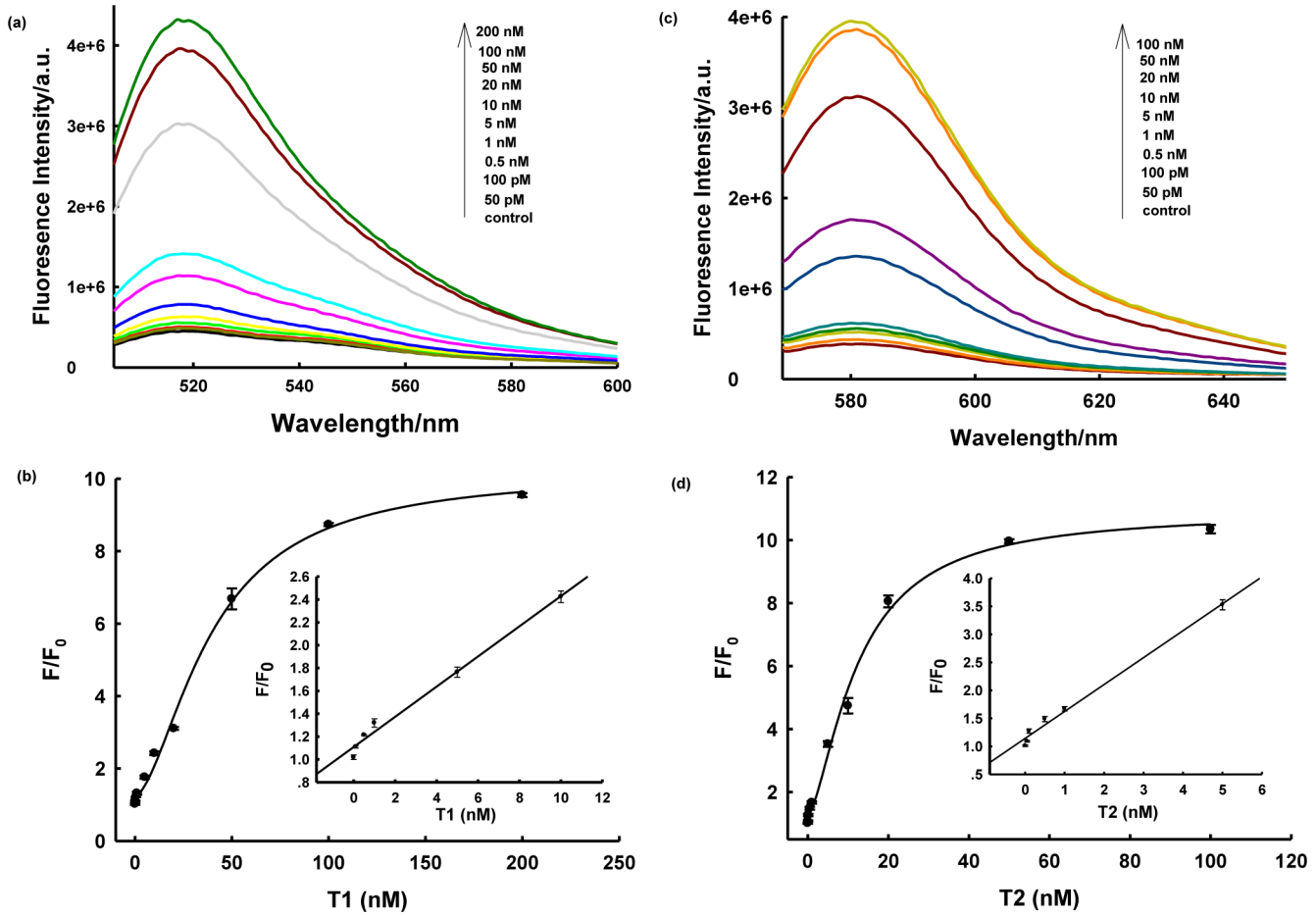

Figure 7. (a) Fluorescence spectra of multiplexed sensing platform at various concentrations of target DNA T1 corresponding to data in the graph. (b) The relationship between fluorescence enhancement and target T1 concentration. (c) Fluorescence spectra of multiplexed sensing platform at various concentrations of target DNA T2 corresponding to data in the graph. (d) The relationship between fluorescence enhancement and target T2 concentration. The data for target T1 were recorded with excitation and emission wavelengths of 559 and 583 nm, respectively. The data for T2 were recorded with excitation and emission wavelengths of 494 and 520 nm, respectively. Inset shows the responses of the sensing system to DNA at low concentration. F_0 and F are the fluorescence intensities of the sensor in the absence and presence of target, respectively.

■ ASSOCIATED CONTENT

Ⓢ Supporting Information

Additional information as noted in text. This material is available free of charge via the Internet at http://pubs.acs.org.

■ AUTHOR INFORMATION

Corresponding Authors

*E-mail: xbzhang@hnu.cn. Phone: +86-731-88821894. Fax: +86-731-88821894.

*E-mail: tan@chem.ufl.edu. Phone: 352-846-2410. Fax: 352-846-2410.

Author Contributions

§R.H. and T.L. contributed equally to this work.

Notes

The authors declare no competing financial interest.

■ ACKNOWLEDGMENTS

This work is supported by grants awarded by the National Key Scientific Program of China (Grant 2011CB911000), NSFC grants (NSFC Grants 21327009, 21325520, 21221003, 21275044, 21205068, J1210040, 21177036, and 21135001), China National Instrumentation Program Grant 2011YQ03012412, and the National Institutes of Health (Grants GM079359 and CA133086).

■ REFERENCES

(1) Risch, N.; Merikangas, K. *Science* **1996**, *273*, 1516.

(2) Liu, G.; Wan, Y.; Gau, V.; Zhang, J.; Wang, L. H.; Song, S. P.; Fan, C. H. *J. Am. Chem. Soc.* **2008**, *130*, 6820−6825.

(3) Cash, K. J.; Heeger, A. J.; Plaxco, K. W.; Xiao, Y. *Anal. Chem.* **2009**, *81*, 656−661.

(4) Liu, G. D.; Lin, Y. H. *J. Am. Chem. Soc.* **2007**, *129*, 10394−10401.

(5) Vaarno, J.; Ylikoski, E.; Meltola, N. J.; Soini, J. T.; Hanninen, P.; Lahesmaa, R.; Soini, A. E. *Nucleic Acids Res.* **2004**, *32*, e108.

(6) Martinez-Manez, R.; Sancenon, F. *Chem. Rev.* **2003**, *103*, 4419−4476.

(7) Borisov, S. M.; Wolfbeis, O. S. *Chem. Rev.* **2008**, *108*, 423−461.

(8) Liu, J.; Cao, Z.; Lu, Y. *Chem. Rev.* **2009**, *109*, 1948−1998.

(9) Gale, P. A. *Chem. Soc. Rev.* **2010**, *39*, 3746−3771.

(10) Xiao, Y.; Qu, X. G.; Plaxco, K. W.; Heeger, A. J. *J. Am. Chem. Soc.* **2007**, *129*, 11896−11897.

(11) Kong, R.; Zhang, X.; Zhang, L.; Huang, Y.; Lu, D.; Tan, W.; Shen, G.; Yu, R. *Anal. Chem.* **2011**, *83*, 14−17.

(12) Zhang, L.; Guo, S.; Dong, S.; Wang, E. *Anal. Chem.* **2012**, *84*, 3568−3573.

(13) Banada1, P. P.; Chakravorty, S.; Shah, D.; Burday, M.; Mazzella, F. M.; Alland, D. *PLoS One* **2012**, *7*, e31126.

(14) Tyagi, S.; Bratu, D. P.; Kramer, F. R. *Nat. Biotechnol.* **1998**, *16*, 49−53.
(15) Dubertret, B.; Calame, M.; Libchaber, A. J. *Nat. Biotechnol.* **2001**, *19*, 365−370.
(16) Yang, R. H.; Jin, J. Y.; Chen, Y.; Shao, N.; Kang, H. Z.; Xiao, Z. Y.; Tang, Z. W.; Wu, Y. R.; Zhu, Z.; Tan, W. H. *J. Am. Chem. Soc.* **2008**, *130*, 8351−8358.
(17) Lu, C. H.; Yang, H. H.; Zhu, C. L.; Chen, X.; Chen, G. N. *Angew. Chem., Int. Ed.* **2009**, *121*, 4879−4881.
(18) Song, S.; Liang, Z.; Zhang, J.; Wang, L.; Li, G.; Fan, C. *Angew. Chem., Int. Ed.* **2009**, *121*, 8826−8830.
(19) Zhao, X. H.; Kong, R. M.; Zhang, X. B.; Meng, H. M.; Liu, W. N.; Tan, W. H.; Shen, G. L.; Yu, R. Q. *Anal. Chem.* **2011**, *83*, 5062−5066.
(20) Song, S. P.; Qin, Y.; He, Y.; Huang, Q.; Fan, C. H.; Chen, H. Y. *Chem. Soc. Rev.* **2010**, *39*, 4234−4243.
(21) Elghanian, R.; Storhoff, J. J.; Mucic, R. C.; Letsinger, R. L.; Mirkin, C. *Science* **1997**, *277*, 1078−1081.
(22) De, M.; Chou, S. S.; Dravid, V. P. *J. Am. Chem. Soc.* **2011**, *133*, 17524−17527.
(23) Mann, J. A.; Alava, T.; Craighead, H. G.; Dichtel, W. R. *Angew. Chem., Int. Ed.* **2013**, *125*, 3259−3262.
(24) Li, J.; Wu, L.; Guo, S.; Fu, H.; Chen, G.; Yang, H. *Nanoscale* **2013**, *5*, 619−623.
(25) Huang, X. L.; Swierczewska, M.; Choi, K. Y.; Zhu, L.; Bhirde, A.; Park, J.; Kim, K.; Xie, J.; Niu, G.; Lee, K. C.; Lee, S.; Chen, X. Y. *Angew. Chem., Int. Ed.* **2012**, *124*, 1657−1662.
(26) Wang, B.; Yu, C. *Angew. Chem., Int. Ed.* **2010**, *49*, 1485−1488.
(27) Kern, J. T.; Kerwin, S. M. *Bioorg. Med. Chem. Lett.* **2002**, *12*, 3395−3398.
(28) Liu, S.; Wang, C.; Zhang, C.; Wang, Y.; Tang, B. *Anal. Chem.* **2013**, *85*, 2282−2288.
(29) Richardson, C. C.; Lehman, I. R.; Kornberg, A. *J. Biol. Chem.* **1964**, *239*, 251−258.
(30) Xuan, F.; Luo, X.; Hsing, I. *Anal. Chem.* **2012**, *84*, 5216−5220.
(31) Xu, Q.; Cao, A.; Zhang, L.; Zhang, C. *Anal. Chem.* **2012**, *84*, 10845−10851.
(32) Jones, R. M.; Bergstedt, T. S.; McBranch, D. W.; Whitten, D. G. *J. Am. Chem. Soc.* **2001**, *123*, 6726−6727.
(33) Murphy, C. B.; Zhang, Y.; Troxler, T.; Ferry, V.; Martin, J. J.; Jones, W. E., Jr *J. Phys. Chem. B* **2004**, *108*, 1537−1543.
(34) Baptista, M. S.; Indig, G. L. *J. Phys. Chem. B* **1998**, *102*, 4678−4688.
(35) Lakowicz, J. R. *Principle of Fluorescence Spectroscopy*; 2nd ed.; Plenum Press: New York, 1999; pp 237−259.
(36) He, Y.; Wang, H.; Yan, X. *Anal. Chem.* **2008**, *80*, 3832−3837.
(37) Chen, L.; McBranch, D. W.; Wang, H.; Helgeson, R.; Wudl, F.; Whitten, D. G. *Proc. Natl. Acad. Sci. U.S.A.* **1999**, *96*, 12287−12292.
(38) Russell, J. C.; Costa, S. B.; Seiders, R. P.; Whitten, D. G. *J. Am. Chem. Soc.* **1980**, *102*, 5678−5679.